Optimal and manufacturable two-dimensional, Kagomé-like cellular solids

S. Hyun and S. Torquato
Princeton Materials Institute and Department of Chemistry, Princeton University, Princeton, New Jersey 08544

(Received 26 April 2001; accepted 25 October 2001)

We used the topology optimization technique to obtain two-dimensional, isotropic cellular solids with optimal effective elastic moduli and effective conductivity. The overall aim was to obtain the best (simplest) manufacturable structures for these effective properties, i.e., single-length-scale structures. Three different but simple periodic structures arose due to the imposed geometric mirror symmetries: lattices with triangular-like cells, hexagonal-like cells, or Kagomé-like cells. As a general rule, the structures with the Kagomé-like cells provided the best performance over a wide range of densities, i.e., for $0 \leqslant \phi < 0.6$, where ϕ is the solid volume fraction (density). At high densities ($\phi > 0.6$), Kagome-like structures were no longer possible, and lattices with hexagonal-like or triangular-like cells provide virtually the same optimal performance. The Kagomé-like structures were found to be a new class of cellular solids with many useful features, including desirable transport and elastic properties, heat-dissipation characteristics, improved mechanical strength, and ease of fabrication.

I. INTRODUCTION

Hashin and Shtrikman found the best possible bounds on the effective elastic moduli[1] and conductivity[2] of isotropic two-phase composites for a given phase volume fraction. Thus, isotropic two-phase composite structures that achieve the bounds are optimal for these properties given volume-fraction information only. Knowledge of such optimal structures is of fundamental and practical value. All of the known optimal structures are multiscale structures[1–7] and therefore not manufacturable. The only exceptions are the single-length-scale structures that achieve the bulk-modulus and conductivity bounds for all volume fractions found by Vigdergauz.[7] The companion shear-modulus bounds are not known to be achievable by simple single-length-scale structures over the entire range of volume fractions.

In a previous study,[8] we determined the elastic moduli of periodic, two-dimensional cellular solids consisting either of triangular or hexagonal cells over the entire range of volume fractions. The triangular honeycombs are actually optimal for the bulk modulus, shear modulus and conductivity in the limit of vanishing solid volume fraction and are close to being optimal for non-zero volume fractions. This work motivates us to ask What are the simplest (i.e., single-length-scale) structures that yield optimal elastic performance?

The purpose of this paper is to identify simple (manufacturable), two-dimensional, isotropic structures that are optimal for the effective bulk and shear moduli over the entire density range. We will focus on single-length-scale periodic structures. This is accomplished with the topology optimization technique[9,10] with a unit cell in which the required elastic isotropic symmetry is enforced by imposing certain geometric mirror symmetries. The topology optimization method has been used to determine the optimal structures of composites for various effective properties without imposing the underlying geometry, i.e., the shape and size of the phase elements and the topology of the individual phases.

In the next section, the Hashin–Shtrikman bounds on the elastic moduli are recalled and discussed. In particular, we briefly describe some of the optimal structures that achieve these bounds. In Sec. III, the topology optimization technique is used to find simple, periodic, two-dimensional, isotropic structures that are optimal for the effective properties. Our results are summarized in Sec. IV. It is shown that at intermediate densities, the optimal structures are characterized by an underlying Kagomé lattice. In Sec. V, we discuss the improved mechanical and transport performance characteristics of Kagomé cellular solids. In Sec. VI, we give concluding remarks and discuss directions for future work.

II. HASHIN-SHTRIKMAN BOUNDS AND OPTIMAL STRUCTURES

A. Hashin–Shtrikman bounds

Consider a two-dimensional isotropic cellular solid that consists of a solid of volume fraction ϕ, bulk modulus k, shear modulus G, and conductivity σ, and a void

 © 2002 Materials Research Society

phase of volume fraction $1-\phi$. Let k_e and G_e be the effective planar bulk and shear moduli, respectively, and σ_e be the effective planar conductivity. The Hashin–Shtrikman upper bounds on the effective moduli of any two-dimensional isotropic cellular solid[1] are given by

$$\frac{k_e}{k} \leqslant \frac{G\phi}{k\,(1-\phi)+G} \quad , \tag{1}$$

$$\frac{G_e}{G} \leqslant \frac{k\phi}{(k+2G)\,(1-\phi)+k} \quad . \tag{2}$$

The corresponding Hashin–Shtrikman upper bound on the effective conductivity[2] is given by

$$\frac{\sigma_e}{\sigma} \leqslant \frac{\phi}{2-\phi} \quad . \tag{3}$$

For reasons of mathematical analogy, results obtained for the effective electrical conductivity translate immediately into equivalent results for the effective dielectric constant, thermal conductivity, and magnetic permeability. Note that the corresponding lower bounds on the moduli and conductivity are essentially zero.

In the low-density limit ($\phi \to 0$), the Hashin–Shtrikman bounds become

$$\frac{k_e}{k} \leqslant \frac{G}{k+G}\phi \quad , \tag{4}$$

$$\frac{G_e}{G} \leqslant \frac{1}{2}\frac{k}{k+G}\phi \quad , \tag{5}$$

$$\frac{\sigma_e}{\sigma} \leqslant \frac{\phi}{2} \quad . \tag{6}$$

We see that the effective properties are linear functions of ϕ. Similarly, in the high-density limit ($\phi \to 1$), the same bounds become

$$\frac{k_e}{k} \leqslant 1 - \frac{k+G}{G}\,(1-\phi) \quad , \tag{7}$$

$$\frac{G_e}{G} \leqslant 1 - 2\,\frac{k+G}{k}\,(1-\phi) \quad , \tag{8}$$

$$\frac{\sigma_e}{\sigma} \leqslant 1 - 2\,(1-\phi) \quad . \tag{9}$$

These asymptotic forms are linear functions of $(1-\phi)$. All two-dimensional isotropic cellular solids must obey bounds (4)–(6) when $\phi \to 0$ and bounds (7)–(9) when $\phi \to 1$.

B. Optimal structures

The Hashin–Shtrikman bounds are the best bounds (i.e., optimal) on k_e, G_e, and σ_e, given only volume-fraction information, because they are known to be attainable by several different types of structures. These include certain multiscale structures, such as space-filling singly coated circles that realize the bulk-modulus[1] and conductivity[2] bounds as well as hierarchical laminates[5,6] that realize the bounds on k_e, G_e, and σ_e. However, such multiscale structures cannot be manufactured. More recently, the bounds on the effective bulk modulus k_e were shown by Vigdergauz[7] to be realizable by simple single-length-scale structures. The same Vigdergauz constructions realize the upper bound on σ_e.

However, simple single-length-scale structures are known only to achieve the shear-modulus upper bound in either the low-density limit ($\phi \to 0$) or the high-density limit ($\phi \to 1$). In the limit $\phi \to 0$, the triangular lattice [Fig. 1(a)] attains the Hashin–Shtrikman upper bounds on both the bulk and shear moduli as well as the conductivity and thus satisfy the asymptotic expressions (4), (5), and (6) as equalities.[12] In this same limit, the Kagomé lattice, a certain combination of the triangular and hexagonal lattice shown in Fig. 1(b), also attains the upper bounds (4), (5), and (6) on both elastic moduli and conductivity.[13] The reasons why these particular structures are optimal are because the elastic response is determined by extension/contraction (not bending) of the cell walls and the transport properties are determined by transport along the cell walls. In the limit $\phi \to 1$, it is well known that dilute arrays of circular holes satisfy the asymptotic expressions (7), (8), and (9). In particular, a dilute array of circular holes arranged on the sites of a hexagonal lattice [Fig. 1(c)] or triangular lattice [Fig. 1(d)] achieve these high-density asymptotic expressions.

III. NUMERICAL SIMULATION USING TOPOLOGY OPTIMIZATION

To find the simplest, periodic, two-dimensional structures (i.e., single-length-scale structures) with optimal elastic moduli, we utilize the conventional topology optimization.[9,10] This numerical optimization technique has been used to determine optimal structures without imposing the underlying topology. This feature is very important because the effective properties of a composite depend sensitively on the connectivity of the phases.

To begin, the design domain is digitized into a large number of finite elements. To simulate infinite systems, we consider a simple unit domain (specified shortly) with periodic boundary conditions. One could begin by making an initial guess for the distribution of the material and void phases among the elements, solve for the local fields using finite elements, homogenize, and then evolve the microstructure to the optimal configuration. However, even for a small number of elements, this integer-type optimization problem becomes a huge and intractable combinatorial problem. Following the idea of standard

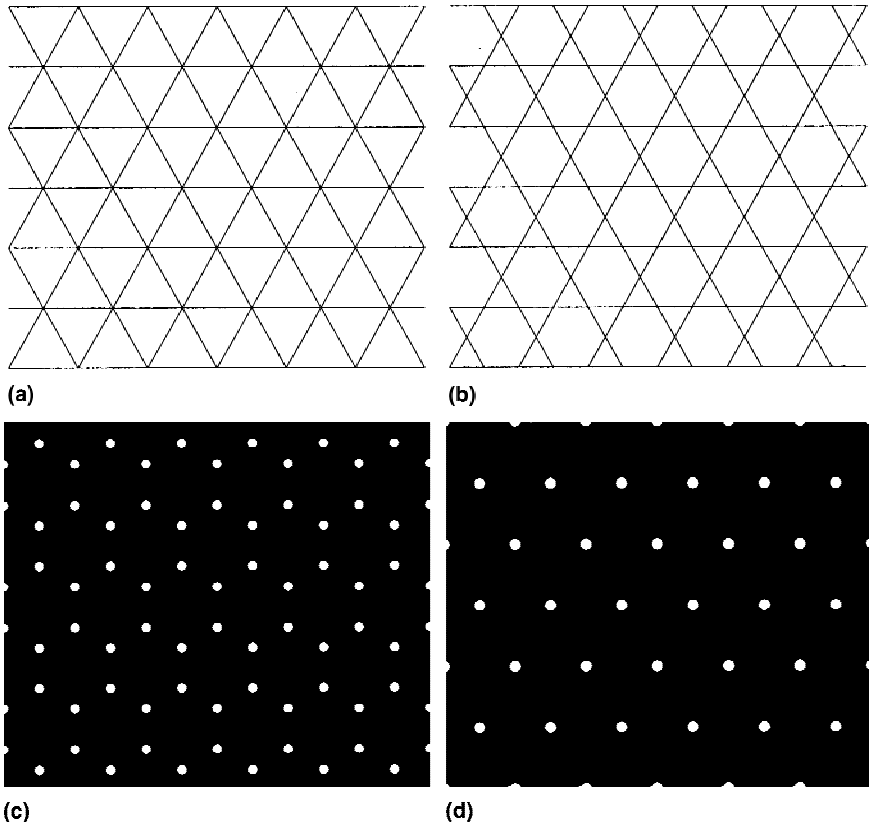

FIG. 1. Examples of optimal two-dimensional, isotropic cellular-solid structures for the effective bulk modulus, shear modulus and conductivity. In the limit $\phi \to 0$, we show (a) the triangular lattice and (b) the Kagomé lattice. In the limit $\phi \to 1$, we show dilute arrays of circular holes centered on the sites of (c) a hexagonal lattice and (d) a triangular lattice.

topology optimization procedures, we relax the problem by allowing the material at a given point to be a grayscale of an intermediate phase that lies between the material phase and void phase.[10,14] In the relaxed system, we let $x_i \in [0, 1]$ be the local density of the ith element, so that when $x_i = 0$, the element corresponds to the void phase and when $x_i = 1$, the element corresponds to the material phase. Let $\mathbf{x}$ $(x_i, i = 1, \ldots, n)$ be the vector of design variables that satisfies the constraint for the fixed volumn fraction $\phi = \langle x_i \rangle$. For any $\mathbf{x}$, the local fields are computed using the finite element method, and the effective property $K_e(K; \mathbf{x})$, which is a function of the material property K and $\mathbf{x}$, is obtained by the homogenization of the local fields. The optimization problem is specified as follows:

$$\text{Maximize} : \Phi = K_e(\mathbf{x}) \quad , \tag{10}$$

$$\text{subject to} : \frac{1}{n}\sum_{i=1}^{n} x_i = \phi \quad ,$$

$$0 \leqslant x_i \leqslant 1, \quad i = 1,\ldots,n \quad ,$$

and prescribed symmetries .

The objective function $K_e(\mathbf{x})$ is generally nonlinear. To solve this problem, we linearize it, enabling us to take advantage of powerful sequential linear programming techniques. Specifically, the objective function is expanded in Taylor series for a given microstructure $\mathbf{x}_0$:

$$\Phi \simeq K_e(\mathbf{x_0}) + \nabla K_e \cdot \Delta\mathbf{x} \quad , \tag{11}$$

where $\Delta\mathbf{x} = \mathbf{x} - \mathbf{x_0}$ is the vector of density changes. In each iteration, the microstructure evolves to the optimal state by determining the small change $\Delta\mathbf{x}$. Following Hyun and Torquato,[15] we use the interior-point method[16] to optimize the linearized objective function in Eq. (11). In each iteration, the homogenization step to obtain the effective property $\mathbf{K}_e(K; \mathbf{x_0})$ is carried out numerically via the finite-element method on the given configuration $\mathbf{x_0}$. Derivatives of the objective function (∇K_e) are calculated by a sensitivity analysis that requires one finite element calculation for each iteration. Refer to Sigmund and Torquato for additional details regarding the topology optimization method.[10]

The objective function Φ is taken to be the effective shear modulus. We use a rectangular unit cell with an aspect ratio of $\sqrt{3}$ (see Fig. 2) for two reasons. First, the required elastic isotropic symmetry can be easily

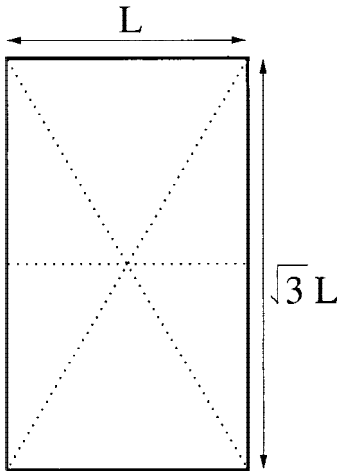

FIG. 2. The unit domain is a rectangle with an aspect ratio of $\sqrt{3}$. This results in structures with hexagonal symmetry, which ensures the structure will be elastically isotropic.

enforced by imposing geometric mirror symmetries about the three lines indicated in Fig. 2. This unit cell in combination with the imposed mirror symmetries result in Bravais lattices having bases with either 3 m (three-fold rotational symmetry axis and one line of mirror symmetry) or 6 mm (six-fold rotational symmetry axis and two lines of mirror symmetry) point group symmetries.[11] For either point group, the elastic symmetry is always isotropic. Second, in our previous work,[8] we found that single-length-scale triangular-cell structures consistent with this unit cell are close to being optimal. The planar bulk modulus k and shear modulus G of the material phase are taken to be 4/3 and 1, respectively. The initial guess for the distribution of phase elements is taken to be random (i.e., the gray scale is assigned randomly) and the structure is evolved to achieve the optimal effective properties under the prescribed constraints. Various filtering parameters[10] were used so that structures with different types of cells could arise. The unit domain was digitized by 82 × 142 square finite elements during the topology optimization process. After the optimization process was completed, the optimized shape was refined by the enhanced resolution of 200 × 346 for the accurate finite element calculation of the effective elastic moduli.

IV. RESULTS

Using the topology optimization technique described in Sec. III, we found periodic, single-length-scale, two-dimensional, isotropic cellular solids with optimal effective shear moduli. Three different but simple periodic structures arise due to the imposed geometric mirror symmetries: structures with triangular-like cells, hexagonal-like cells, or Kagomé-like cells. Whereas the triangular-like and hexagonal-like structures are characterized by cells of the same shape and size, the Kagomé-like structures are characterized by cells of two different shapes and sizes (large hexagonal-like cells and smaller triangular-like cells). The cell sizes were controlled by changing the filtering parameter in the topology optimization technique. We obtained results for a wide range of volume fractions: ϕ = 0.1, 0.2. 0.3, 0.4, 0.5, 0.6, 0.7, 0.8, and 0.9. Our optimization results for the effective shear modulus are summarized in Fig. 3. The corresponding effective bulk moduli amid conductivities for these optimal structures were directly computed and are summarized in Figs. 4 and 5. We note that the optimal structures for the shear modulus tend to be optimal for the bulk modulus and conductivity as well. As a general rule, the structures with the Kagomé-like cells yield the best performance over a wide range of densities, i.e., for $0 \leqslant \phi < 0.6$, where ϕ is the solid volume fraction (density). At high densities ($\phi > 0.6$), Kagomé-like

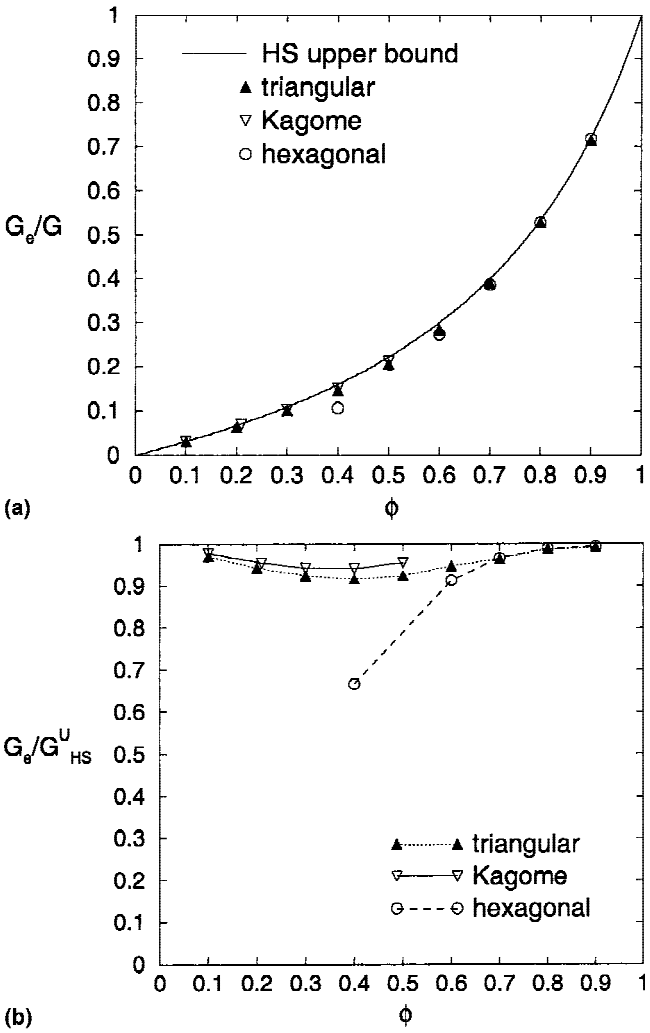

FIG. 3. The dimemisionless effective shear modulus G_e/G versus solid volume fraction ϕ for the optimal single- and double-length-scale structures that we found by the topology optimization method. The Hashin–Shtrikman upper bound (2) is included.

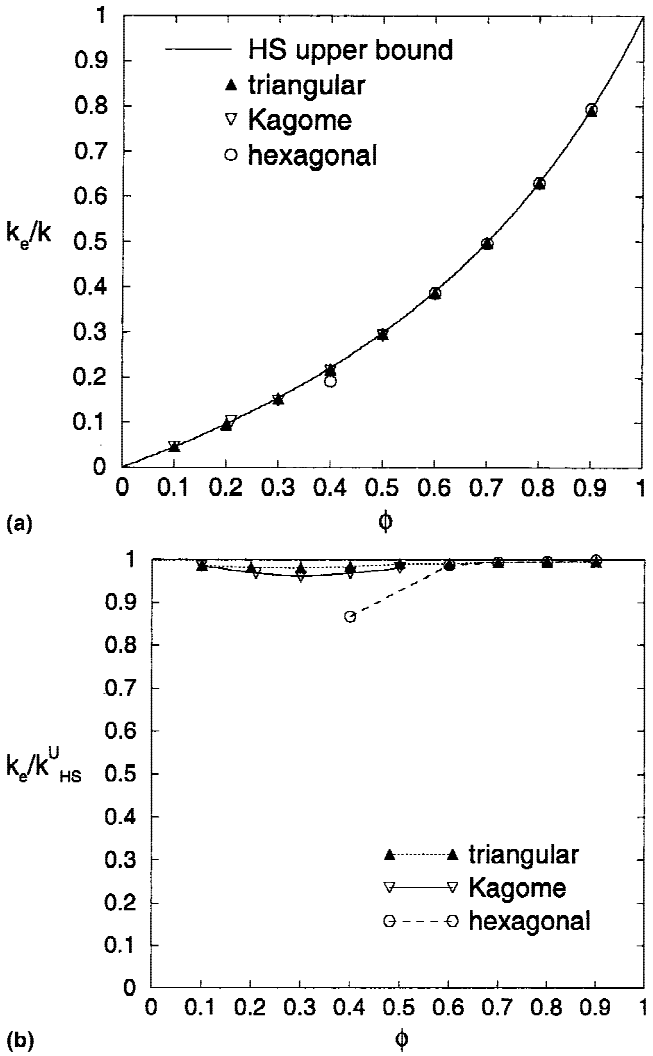

FIG. 4. The dimensionless effective bulk modulus k_e/k versus solid volume fraction ϕ corresponding to the optimal shear-modulus structures of Fig. 3. The Hashin–Shtrikman upper bound (1) is included.

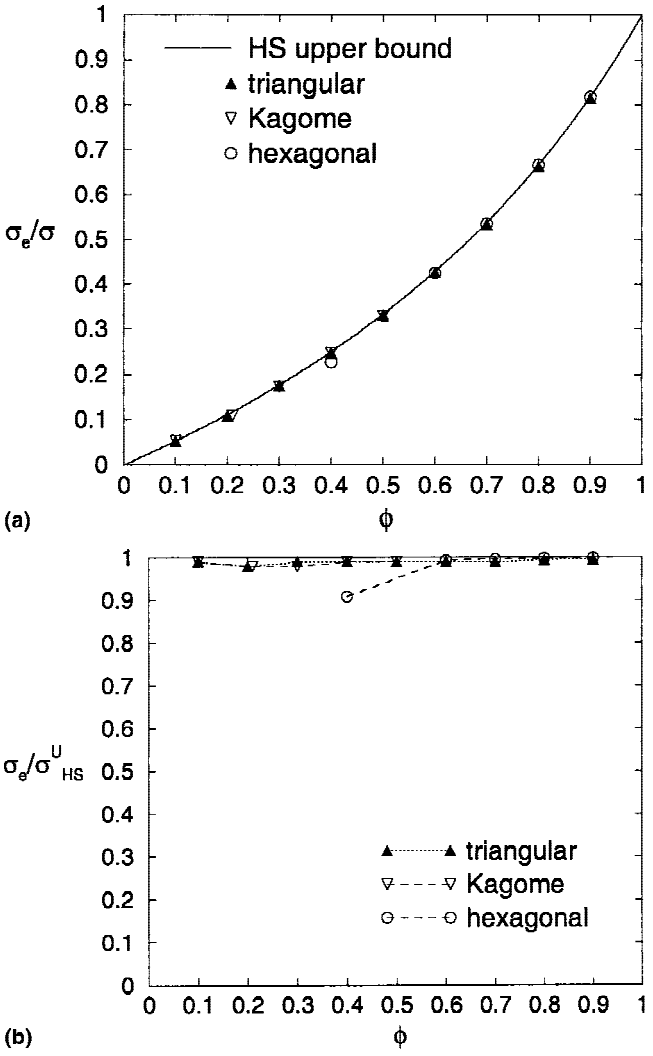

FIG. 5. The dimensionless effective conductivity σ_e/σ versus solid volume fraction ϕ corresponding to the optimal shear-modulus structures of Fig. 3. The Hashin–Shtrikman upper bound (3) is included.

structures are no longer possible and lattices with hexagonal-like or triangular-like cells provide virtually the same optimal performance.

We have already noted that as the density goes to zero ($\phi \to 0$), both the triangular and Kagomé lattices (see Fig. 1) are optimal for the shear modulus (as well as bulk modulus and conductivity) among all structures; i.e., they achieve the Hashin–Shtrikman upper bounds (4)–(6). Thus, it comes as no surprise that at finite but low densities ($\phi = 0.1$), both the triangular-like cell structures and Kagomé-like cell structures are virtually the same as the Hashin–Shtrikman upper bounds. (Note that the centers of the triangular-like cells are situated on the sites of a hexagonal lattice.) Figure 6 shows both of these optimal structures at $\phi = 0.1$.

However, at intermediate densities ($0.3 \leqslant \phi < 0.6$), the Kagomé-like cell structures are superior to the triangular-like cell structures. Figures 7 and 8 show the resulting optimal structures at $\phi = 0.3$ and 0.5. At $\phi = 0.5$, for example, the effective shear modulus of the triangular-like and Kagomé-like cell structures are 93% and 96% of the Hashin–Shtrikman upper bound (see Fig. 3). Both of these optimal shear-modulus structures are up to 98–99% of the Hashin–Shtrikman upper bounds on the bulk modulus and conductivity (see Figs. 4 and 5). Thus, although Kagomé-like cell structures are suboptimal in that they have effective properties that lie below (but close to) the Hashin–Shtrikman upper bounds, they are the optimal, single-length-scale structure.

At high densities ($0.7 \leqslant \phi < 1$), the structures with the triangular-like or hexagonal-like cells offer the best performance. Specifically, at $\phi = 0.7$, triangular-like cells (with smoothed corners), with centers on the sites of a hexagonal lattice, and circular-like cells on the sites

of a triangular lattice are the optimal structures for the elastic moduli and conductivity (see Fig. 9). At $\phi = 0.9$, the cell shapes approach a circle on either a hexagonal or triangular lattice (see Fig. 10) and possess properties that approach the Hashin–Shtrikman upper bounds. This is consistent with the earlier observation (given in Sec. II) that dilute arrangements of circles are optimal among all structures, i.e., they achieve the Hashin–Shtrikman upper bounds (7)–(9). Note that at the high densities ($\phi > 0.6$), the Kagomé-like structures are not attainable.

Vigdergauz[7] used a genetic algorithm to find the optimal shapes of single-size cells centered on the sites of a triangular lattice for the effective shear modulus. At the solid volume fraction $\phi = 0.4$, he found that the optimal cell shape was hexagonal-like. This structure is compared to the optimal Kagomé-like cell structure that we found in the present study in Fig. 11. The effective moduli of the Kagomé-like cell structure are about 95% of the Hashin–Shtrikman upper bounds and therefore are significantly higher than the effective moduli of the structure found by Vigdergauz (about 65% of the Hashin–Shtrikman upper bounds); see Fig. 3 at $\phi = 0.4$. Of course, in the high density range, the optimal cell shapes that Vigdergauz found become circular-like, and in the limit $\phi \to 1$, become circles, which we have seen are optimal among all shapes.

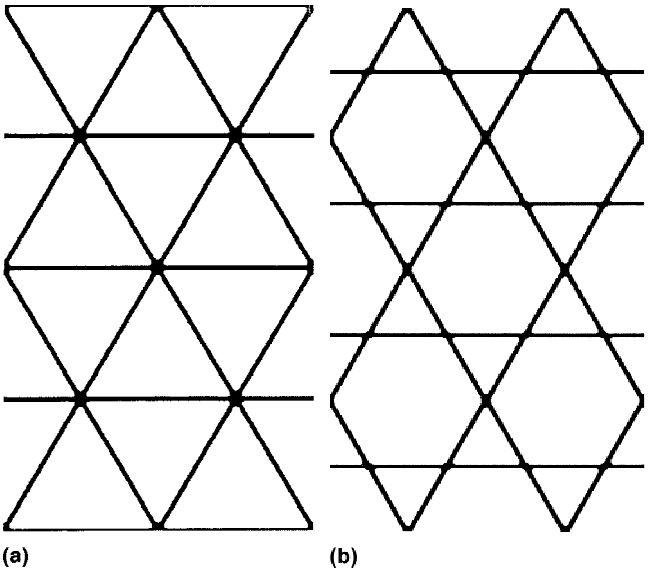

FIG. 6. Optimal structures that we found for the effective shear modulus at $\phi = 0.1$. Shown are two-by-two arrays of the optimal unit cells.

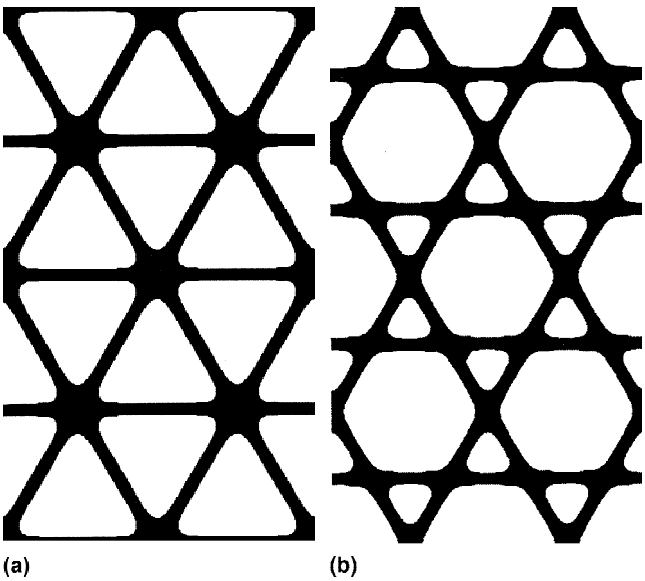

FIG. 7. As in Fig. 6, except that $\phi = 0.3$.

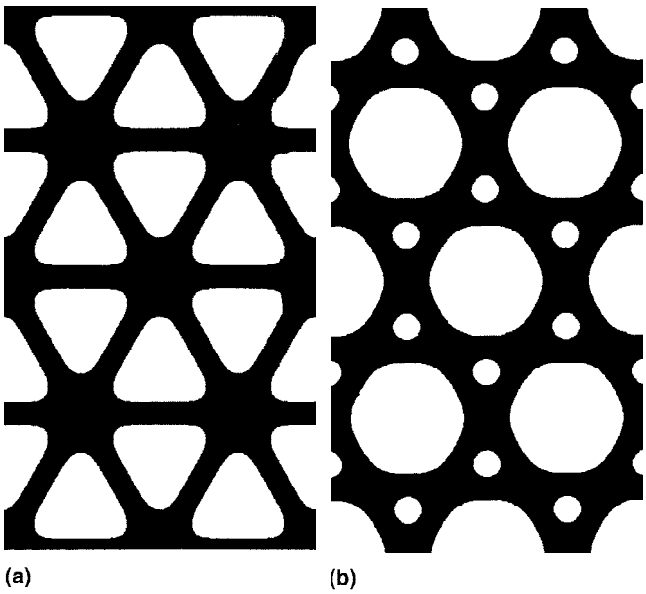

FIG. 8. As in Fig. 6, except that $\phi = 0.5$.

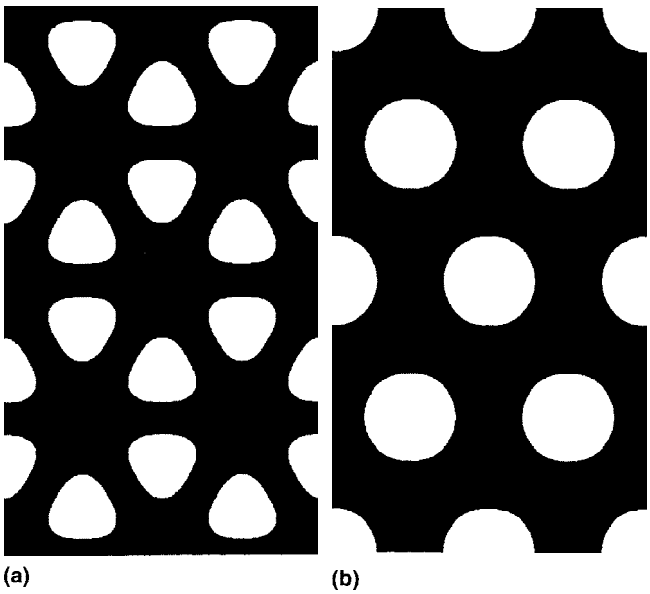

FIG. 9. As in Fig. 6, except that $\phi = 0.7$.

V. KAGOMÉ CELLULAR SOLID AS A MULTIFUNCTIONAL MATERIAL

Since Syozi[18] introduced the Kagomé lattice for the study of phase transitions in magnetic materials, this lattice has been investigated to understand its interesting magnetic properties,[19–21] superconducting properties,[22] as well as its percolation characteristics.[23] However, there have been only a few studies of its macroscopic properties when used as a cellular solid, although, as we will see, the Kagomé lattice possesses interesting features and may find useful applications. Chen *et al.*[24] examined the percolation behavior of the elastic constants for the Kagomé lattice. Except for the observation that the Kagomé lattice has optimal elastic moduli in the zero-density limit,[13] its desirability as a material with useful multifunctional characteristics has heretofore not been pointed out.

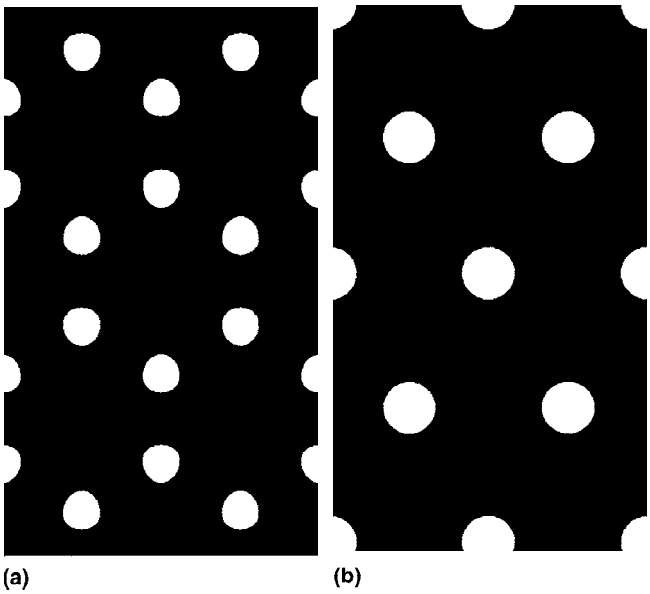

FIG. 10. As in Fig. 6, except that $\phi = 0.9$.

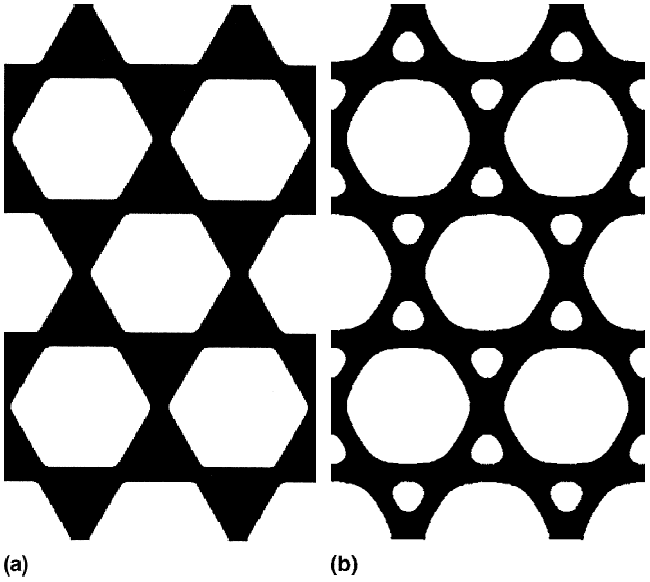

FIG. 11. Optimal hexagonal-like cellular structure (a) found by Vigdergauz[17] and optimal Kagomé-like cellular structure (b) found by us for the effective shear modulus at the volume fraction $\phi = 0.4$. Structures (a) and (b) achieve about 65% and 95% of the Hashin–Shtrikman upper bound, respectively.

Our identification of Kagomé-like cellular solids as simple but optimal structures in their elastic moduli and transport properties for an appreciable range of volume fractions suggest that such materials may have other useful properties. For example, Kagomé-like cellular solids will have superior strength to the elastic buckling loads than either triangular-like or hexagonal-like cellular solids. We performed finite element calculations to compare the strengths of triangular-like structures and Kagomé-like structures under the Euler buckling loads at the low volume fraction of $\phi = 0.1$ (see Fig. 6). The local axial stresses (σ_{axial}) along the centroids of the cell walls (horizontal cell walls) were calculated under external uniaxial (horizontal and vertical) and shear loads. We compared only the axial stresses because the elastic responses are determined by extension/contraction (not bending) of the cell walls at such a low density. As seen in the Table I, these two cellular solids have virtually the same local stresses in the corresponding cell walls under the same external loading conditions.

From standard beam theory,[25] when the thickness of the walls is constant and the length of the walls is λ, the critical Euler buckling load P_{crit} is given by

$$P_{crit} = \frac{n^2 \pi^2 E_s I}{\lambda^2} \quad , \tag{12}$$

where E_s is the Young's modulus of the solid phase, and I is the second moment of inertia of the cell wall. The factor n describes the rotational stiffness of the node where the cell walls meet. It is seen that the length of a cell wall in the Kagomé lattice is half of that in the triangular lattice [Figs. 6(a) and 6(b)]. Thus, Kagomé-like cellular solids can be made four times more resistant to the same elastic buckling loads than the triangular cellular solid.

TABLE I. Local axial stresses (σ_{axial}) along the centroids of the cell walls of the triangular-like and Kagomé-like cellular solids (due to unit external stresses) at a volume fraction $\phi = 0.1$. Horizontally oriented cell walls (A) as well as cell walls oriented at 60 degrees with respect to the horizontal (B) are considered.

	Triangular-like		Kagomé-like	
External loading	cell wall A	cell wall B	cell wall A	cell wall B
Horizontal	2.374	0.6081	2.395	0.6049
Vertical	0.01422	1.845	0.01093	1.835
Shear	−0.00024	1.066	0.00146	1.050

Although multiscale or hierarchical structures may have optimal properties, they are not usually manufacturable, or high cost is required to fabricate them. However, Kagomé-like structures could be manufactured easily. For example, man has made use of this particular structure to fabricate (bamboo) baskets (which the lattice was originally named after).[18] Kagomé-like structures can be manufactured relatively easily by weaving metallic wires. This textile-based approach has been used to fabricate square networks in multifunctional microtruss laminates.[26] Our present work suggests that the Kagomé pattern can be used in the same sandwich panels to improve the aforementioned mechanical performances. Indeed, besides the textile-based technique, a rapid prototyping and investment casting technique has been utilized to fabricate more complicated structures, such as the tetragonal[27] and three-dimensional Kagomé patterns in truss core panels.[28]

Besides having desirable mechanical and conduction properties, Kagomé-like cellular solids will have desirable heat-dissipation properties due to the large hexagonal holes through which fluid may flow [see Fig. 6(b)]. It is known that hexagonal holes provide much higher heat-dissipation performance than triangular holes in sandwich panels with two-dimensional metal cores.[29] Thus, Kagomé-like cellular solids may find useful applications as a multifunctional material at both macroscopic and microscopic levels.

VI. CONCLUSIONS

We have identified the single-length-scale, two-dimensional, isotropic, cellular solids that are optimal for the elastic moduli and transport properties over the entire range of volume fractions. Structures with Kagomé-like cells are found to be a new class of cellular solids with many useful features, including desirable transport and elastic properties, heat-dissipation characteristics, improved mechanical strength, and ease of fabrication. We recall that none of the obtained structures in this study achieves the Hashin–Shtrikman upper bounds in the intermediate-density range. Although our numerical procedure does not rigorously prove that single-length-scale structures cannot achieve the Hashin-Shtrikman upper bounds on the bulk and shear moduli and conductivity, it suggests that this may be the case. It has recently been shown that the nonlinear mechanical behavior of Kagomé core panels are superior to tetragonal core panels.[28]

ACKNOWLEDGMENTS

The authors thank A.G. Evans and A.M. Karlsson for very useful discussions, and S. Vigdergauz for providing his optimum shape. They also gratefully acknowledge the support of the Office of Naval Research under Grant No. N00014-00-1-0438.

REFERENCES

1. Z. Hashin and S. Shtrikman, J. Mech. Phy. Solids **11,** 127 (1963); Z. Hashin, J. Mech. Phys. Solids **13,** 119 (1965).
2. Z. Hashin and S. Shtrikman, J. Appl. Phys. **33,** 3125 (1962).
3. K.A. Lurie and A.V. Cherkaev, J. Opt. Theor. Appl. **46,** 571 (1985).
4. A.N. Norris, Mech. Mater. **4,** 1 (1985).
5. G.W. Milton, in *Homogenization and Effective Moduli of Materials and Media*, edited by J.L. Eriksen, D. Kinderlehrer, R. Kohn, and J.L. Lions (Springer-Verlag, New York, 1986).
6. G.A. Francfort and F. Murat, Arch. Rat. Mech. Anal. **94,** 307 (1986).
7. S.B. Vigdergauz, Mech. Solids **24,** 57 (1989); S.B. Vigdergauz, J. Appl. Mech. **3,** 300 (1994).
8. S. Hyun and S. Torquato, J. Mater. Res. **15,** 1985 (2000).
9. M.P. Bendsoe and N. Kikuchi, Comp. Meth. Appl. Mech. Eng. **71,** 197 (1988).
10. O. Sigmund and S. Torquato, J. Mech. Phys. Solids **45,** 1037 (1997).
11. C. Kittel, *Introduction to Solid State Physics*, 2nd ed. (John Wiley & Sons, New York, 1956).
12. S. Torquato, L.V. Gibiansky, M.J. Silva, and L.J. Gibson, Int. J. Mech. Sci. **40,** 71 (1998).
13. R.M. Christensen, Int. J. Solids Struc. **37,** 93 (2000).
14. M.P. Bendsoe and O. Sigmund, Arch. Appl. Mech. **69,** 635 (1999).
15. S. Hyun and S. Torquato, J. Mater. Res. **16,** 280 (2001).
16. N. Karmarkar, Combinatoria **4,** 373 (1984).
17. S. Vigdergauz (unpublished).
18. I. Syozi, Prog. Theor. Phys. **VI,** 306 (1951).
19. P.W. Anderson, Phys. Rev. **102,** 1008 (1956).
20. G. Aeppli and P. Chandra, Science **275,** 177 (1997).
21. I.S. Hagemann, Q. Hunag, X.P.A. Gao, A.P. Ramirez, and R.J. Cava, Phys. Rev. Lett. **86,** 894 (2001).
22. M.J. Higgins, Y. Xiao, S. Bhattacharya, P.M. Chaikin, S. Sethuraman, R. Bojko, and D. Spencer, Phys. Rev. Lett. **61,** R894 (2000).
23. S. Torquato, *Random Heterogeneous Materials: Microstructure and Macroscopic Properties* (Springer-Verlag, New York, 2002).
24. J. Chen, M.F. Thorpe, and L.C. Davis, J. Appl. Phys. **77,** 4349 (1995).
25. L.J. Gibson and M. Ashby, *Cellular Solids*, 2nd ed. (Pergamon Press, New York, 1997).
26. D.J. Sypeck and H.N.G. Wadley, J. Mater. Res. **16,** 890 (2001).
27. S. Chiras, D.R. Mumm, A.G. Evans, N. Wicks, J.W. Hutchinson, K. Dharmasena, H.N.G. Wadley, and S. Fichter, Int. J. Solids Struct. (in press).
28. S. Hyun, A.M. Karlsson, S. Torquato, and A.G. Evans (unpublished).
29. S. Gu, T.J. Lu, and A.G. Evans (unpublished).